

Low Temperature Photoluminescence Characteristics of Chemically Synthesized Indium Doped Zinc Oxide Nanostructures

A. Escobedo Morales¹, R. Aceves², U. Pal^{1,*}, and J. Z. Zhang³

¹Instituto de Física, Benemérita Universidad Autónoma de Puebla, Apdo. Postal J-48, CP 72570, Puebla, Pue., México

²Centro de Investigación en Física, Universidad de Sonora, Apdo Postal: 5-48, CP 83190, Hermosillo, Sonora, México

³Department of Chemistry and Biochemistry, University of California, Santa Cruz, CA 95064, USA

Photoluminescence (PL) emission and excitation (EPL) spectra of un-doped and indium (1%) doped 1D zinc oxide nanostructures are studied at different temperatures. The nanostructures reveal a blue emission band attributed to localized donor states. Indium doping enhances the blue emission. While at low temperatures (<50 K) PL spectra are dominated by the emission attributed to the recombination of excitons bound to neutral donors (D^0, X), at higher temperatures (>100 K), defect related emissions in the visible range dominate over the excitonic emission. Temperature dependence measurements on the doped sample reveal that (D^0, X) emission energies obey the Varshni's formula with fitting constants $\alpha = 8.4 \pm 0.3 \times 10^{-4}$ eV/K and $\beta = 650 \pm 40$ K. The (D^0, X) emission intensity decays exponentially with temperature.

Keywords: Zinc Oxide, Nanostructures, Indium-Doping, Photoluminescence.

1. INTRODUCTION

Throughout the last decade, the interest on light emitting semiconductors with a wide band gap was focused on GaN.¹ However, in recent years considerable effort has been made to develop a new generation of optoelectronic devices based on II–VI semiconductors. In this regard, zinc oxide (ZnO) has been one of the most promising compounds, due to its desirable electronic properties like a direct band gap of 3.37 eV at room temperature,² and larger exciton binding energy (60 meV)³ than GaN (25 meV).⁴ Since its exciton binding energy is beyond the thermal energy at room temperature (25 meV),⁵ it opens up the possibility to obtain ultraviolet lasing response without the necessity of cryogenic temperatures or high excitation energies.⁶ Nevertheless, high quality crystals are required to generate the lasing effect. Scientists believe that an alternative route to obtain higher optical emissions is using doped semiconductor nanostructures, as these low-dimensional materials facilitate lasing effect due to enhanced density of states near their band edges.⁷ Therefore, efforts to incorporate shallow states in the electronic band structure of ZnO bulk and nanostructures by introducing doping atoms in the host lattice have

been carried out.^{8–10} It is well known that upon doping, structural defects that appear in the lattice could result in radiative or non-radiative centers in the nanostructures. Beside the extrinsic defects, the effect of native defects on the luminescent properties of ZnO structures has been extensively studied.^{11–13} Nevertheless, not all its optical characteristics are clear, and there is still controversy on the origin of visible emissions in their luminescence spectra. By far, the green luminescence band is the most common visible emission observed in bulk ZnO, and has been attributed to the single ionized oxygen vacancies V_o^+ .¹⁴ On the other hand, yellow, red, and blue emissions have also been observed in undoped zinc oxide,¹⁵ and their origin still requires further studies.

Here we report the photoluminescence of undoped and indium doped rod-like zinc oxide nanostructures grown by hydrothermal technique. Distinct temperature and excitation evolution of the donor bound exciton (D^0, X), and blue emissions in undoped and doped nanostructures are observed. On the basis of the observed results, possible mechanisms for such emissions are discussed.

2. EXPERIMENTAL DETAILS

Undoped and indium doped zinc oxide nanostructures were obtained by hydrolysis in an alkaline aqueous

*Author to whom correspondence should be addressed.

solution, as described earlier.¹⁶ In a typical synthesis process, an alkaline solution was prepared by dissolving 12 ml of ethylenediamine ($\text{NH}_2(\text{CH}_2)_2\text{NH}_2$, EDA; Baker, 99.9%) in 108 ml of ultra pure deionized water (18.0 M Ω cm). To the previous solution, 10.25 g of zinc acetate dihydrate ($\text{Zn}(\text{CH}_3\text{COO})_2 \cdot 2\text{H}_2\text{O}$; Aldrich, 99.99%) in powder form was added, followed by the addition of 1.70 g of sodium hydroxide (NaOH; Aldrich, 99.99%). The hydrothermal synthesis was conducted at 90 °C for 15 h in a round bottom flask using an oil bath for heating. After cooling to room temperature, the white material adhered to the reaction flask wall was extracted by decantation and dried in a muffle furnace at 80 °C for 2 h after washing by deionized water several times. For doping, 0.1034 g of indium chloride (III) powder (InCl_3 ; Adrich, 99.999%) was added to the reaction mixture before heating, to prepare nominal 1% indium doped ZnO nanostructures. After the hydrothermal synthesis, the samples were annealed in a horizontal furnace (Lindberg/Blue, model V0914A) at 300 °C for 9 h in an argon atmosphere. Photoluminescence of the ZnO nanostructures were measured at different temperatures in a fluorescence spectrophotometer equipped with a 450 W Xe lamp (Fluorolog, Jovin Yvon) and a close-cycle He cryostat (HC-2, APD Cryogenics). Lattice structure and morphology of the samples were studied by X-ray diffraction (XRD) (Phillips X'Pert diffractometer with Cu K α radiation), and scanning electron microscopy (SEM) (Jeol JSM 5300). Composition of the samples was measured by

energy dispersive spectroscopy (EDS) with the analytical system attached with the scanning electron microscope. For obtaining the composition, EDS spectra were recorded at different places of the samples and the results were averaged.

3. RESULTS AND DISCUSSION

The SEM micrographs (Fig. 1) revealed a needle-like morphology for both the In doped and undoped samples. The diameter and length of the nanostructures varied from 250 to 500 nm and 3 to 6 μm , respectively. Formation of some particles, along with the needle-like structures in In doped samples are observed (shown by an arrow). X-ray diffraction (XRD) patterns of the samples (Fig. 1) revealed characteristic wurtzite lattice features of zinc oxide (JCPDS 36-1451). There appeared no diffraction peak in the doped sample that can be related to any other phase than ZnO. While the energy dispersive spectroscopy (EDS) revealed almost a perfect stoichiometry (Zn and O atomic ratio close to 1) for the undoped nanostructures, it revealed 48.5 atom% of Zn, 50.3 atom% of O and about 1.2 atom% of In for the In doped sample.

The PL spectra shown in Figure 2 were recorded at 15 K using 325 nm, 350 and 360 nm excitations. All the PL spectra are dominated by a narrow emission band located at about 369 nm (3.360 eV). The emission can be attributed to the recombination of excitons bound to

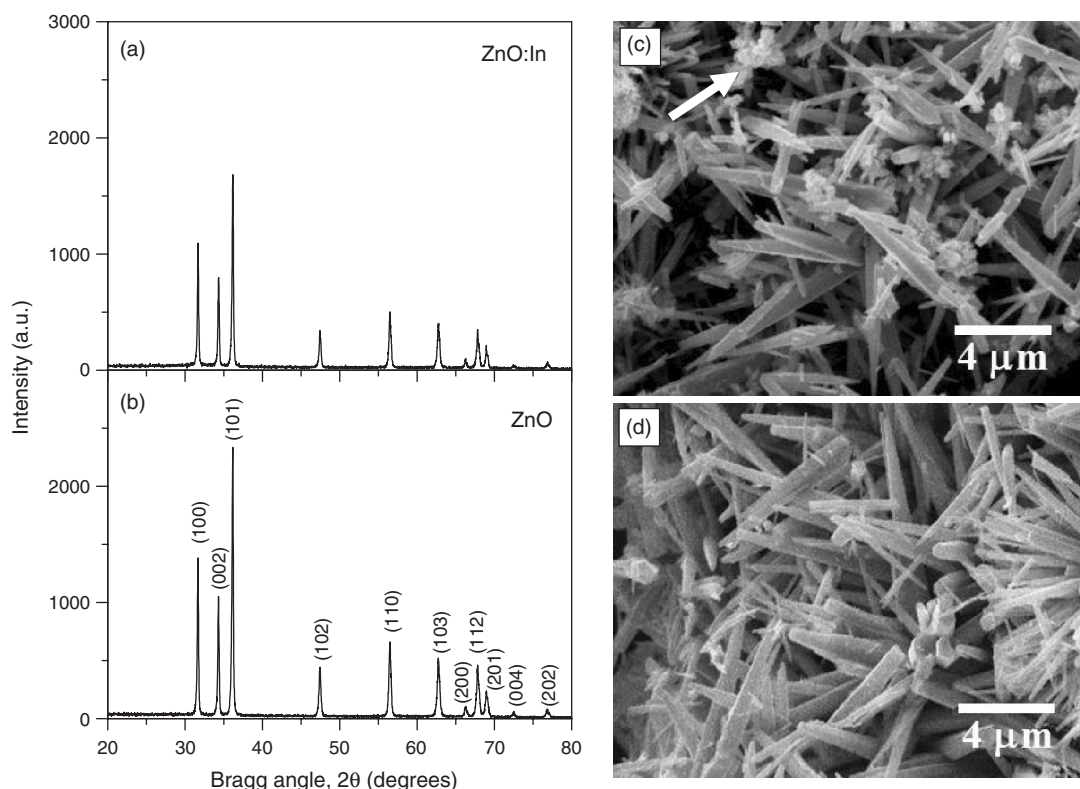


Fig. 1. XRD pattern and SEM micrographs of the annealed undoped (a, c) and doped (b, d) zinc oxide samples.

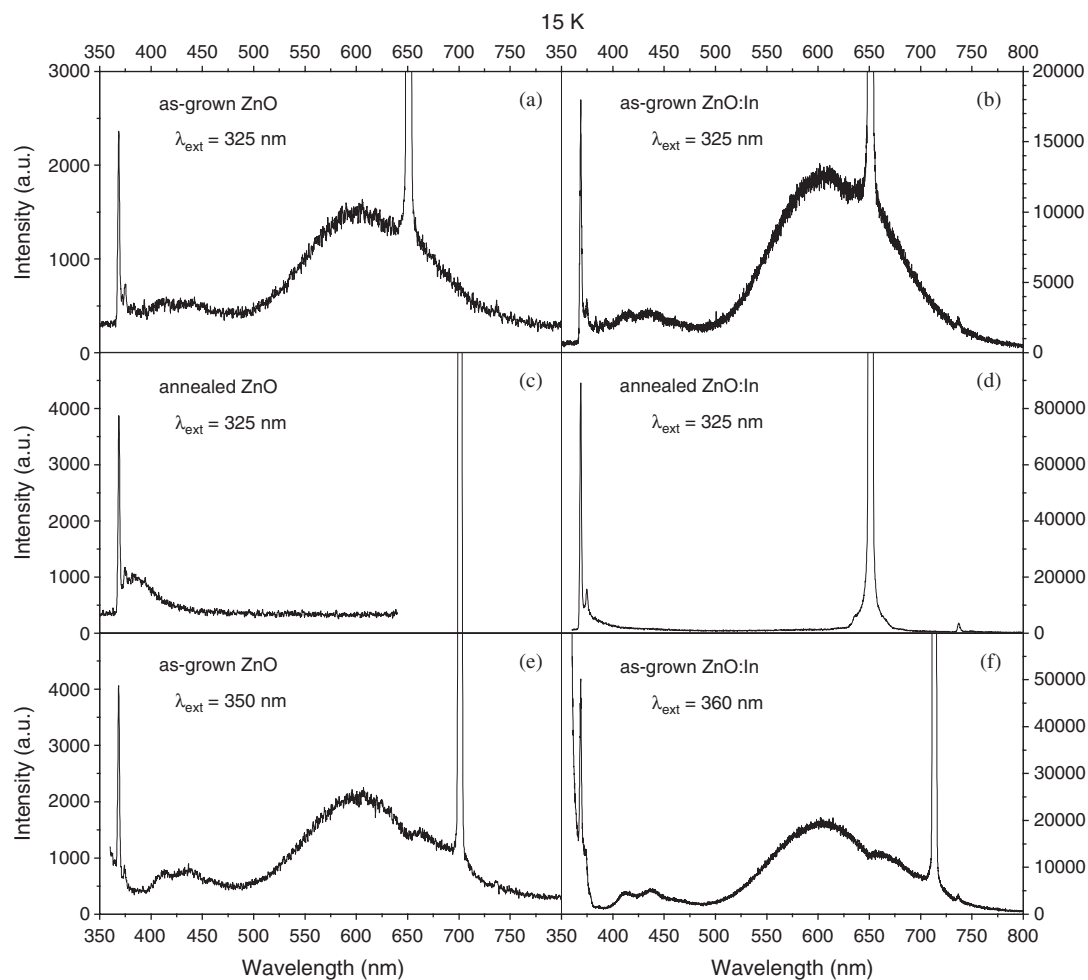


Fig. 2. PL spectra of as-grown (a, b) and annealed (c, d) samples at 15 K. The sharp peak in the red is due to the second order Rayleigh scattering of the excitation light.

neutral donors (D^0, X),^{17–20} like Zn_i^0 and V_o^0 .²¹ Surprisingly, a band at about 368 nm has been observed for In doped nanostructured ZnO thin films, but not in undoped films, by Chen et al.²² A second narrow band near the exciton emission appears near 375 nm (3.306 eV); about 73 meV below the position where the free exciton emission at 15 K (FX, 3.379 eV) for ZnO is expected.²³ As the energy shift matches with the LO phonon energy for ZnO,²⁰ the emission could be assigned to the free exciton first phonon replica (1LO-FX).¹⁷

It is worth to note that the exciton recombination band does not change its position on indium incorporation, indicating no significant change in band gap. This suggests that indium impurity levels are located very close to the conduction band edge. However, indium doping has a clear influence on the intensity of the (D^0, X) emission. On indium doping, the intensity of the (D^0, X) emission increases. The effect is more evident in the annealed samples, where the intensity for In doped ZnO is about twenty times higher than that of undoped sample. As an annealing process enhances the crystal quality and stimulates the

incorporation of indium in lattice sites though substitution (In_{Zn}),¹⁶ formation of bound excitons in indium doped samples is expected to be enhanced.

In the region between 400 nm and 450 nm (blue region), two weak emission bands at about 413 (3.0 eV) and 436 nm (2.84 eV) appeared for the un-annealed sample. After the annealing process, the bands disappeared. Instead, a weak band in the UV region (~ 384 nm, 3.22 eV) arises as the hump of the (D^0, X) emission. Appearance of this weak emission in annealed samples suggests the presence of shallow trap states near the bottom of the conduction band, probably due to the formation of zinc interstitial (Zn_i) or oxygen vacancy (V_o) related defects generated by thermal annealing. While the band at about 436 nm has been assigned as the blue emission in ZnO earlier, very recently, De la Rosa et al.²⁴ have also assigned the other band as blue emission. The blue emission (2.84 eV) which disappears after thermal annealing could be revealed while exciting the samples at shorter wavelengths (discussed latter). For the moment, the origin of the emission band at about 3.0 eV is not very clear. We suggest that this emission comes from

the transition of the trapped electrons at the shallow oxygen vacancy (V_o) levels to the valence band.

For the as-grown samples (Fig. 2), two broad bands appear clearly in the region attributed to the deep level emissions (500–800 nm). The first band, located at about 607 nm (2.04 eV), is known as yellow emission in ZnO. Wu et al. proposed that the single negatively charged interstitial oxygen (O_i^-) is responsible for the yellow luminescence.^{25,26} While the band remains at its position, its intensity increases about ten times on indium doping. We believe this emission is due to the transition between shallow defect levels and a deep level. Wu et al.²⁵ have suggested that this emission is produced by the recombination of delocalized electrons close to the conduction band with deeply trapped holes in the O_i^- point defect level. We have observed a similar increase of yellow emission intensity in indium doped ZnO nanostructures in their CL spectra.²⁷ The second band, located at around 660 nm (1.87 eV) and superimposed with the first harmonic of the 325 nm excitation for both doped and undoped samples, is the so-called red emission of ZnO. The intensity of this emission is higher for the doped sample. Presence of this band is clearer in the Figures 2(e and f), where the samples were excited with longer wavelengths. After annealing, the intensity of this band reduces drastically. In fact, both the yellow and red emissions become imperceptible for the doped and undoped samples after the annealing process. The red emission has been related to the interstitial zinc which causes a lattice disorder in ZnO along c -axis,²⁸ introducing shallow donor levels.²⁹ On the other hand, Studenikin et al.³⁰ attributed this emission to the amount of interstitial oxygen in their oxygen rich ZnO samples. As the position of this band did not change with

indium doping, it seems that the band could originate from a donor acceptor pair (DAP) transition.

In order to study the characteristics of the (D^0,X) and blue emission bands in ZnO in details, PL emission spectra of the annealed samples were recorded at different temperatures in between 15 and 300 K, using a 280 nm excitation source. This excitation wavelength was chosen because at such photon energy the blue emission is enhanced as revealed in the excitation photoluminescence (PLE) spectra of the sample (discussed latter). The temperature dependent PL spectra for the annealed undoped and indium doped samples are shown in Figure 3.

It can be noticed that the (D^0,X) emission intensity decreases faster than the 1LO-FX emission as the temperature increases. Such a rapid decrease of (D^0,X) emission intensity is due to weak binding between excitons and donor defects at higher temperatures. Distinct temperature variations of the (D^0,X) and 1LO-FX emission intensities also support that the emission located at 375 nm is not the 1LO-DX, since it is expected that with the increase of temperature, both (D^0,X) emission and its phonon replica should quench in a similar way. Figure 4 resumes the temperature dependence of (D^0,X) emission intensity, which decays exponentially with the increase of temperature. It is found that the intensity decay curve follows the expression:

$$I = I_0 e^{E_a/kT} \quad (1)$$

where $I_0 = 1930$, $E_a = 3.9$ meV. The other characteristic of the (D^0,X) emission is the variation of its position with temperature. It is possible to apply the Varshni's formula³¹ to fit the position of the (D^0,X) energy with temperature, as shown in Figure 4. Since the binding energy of exciton is considered to be nearly independent of temperature for

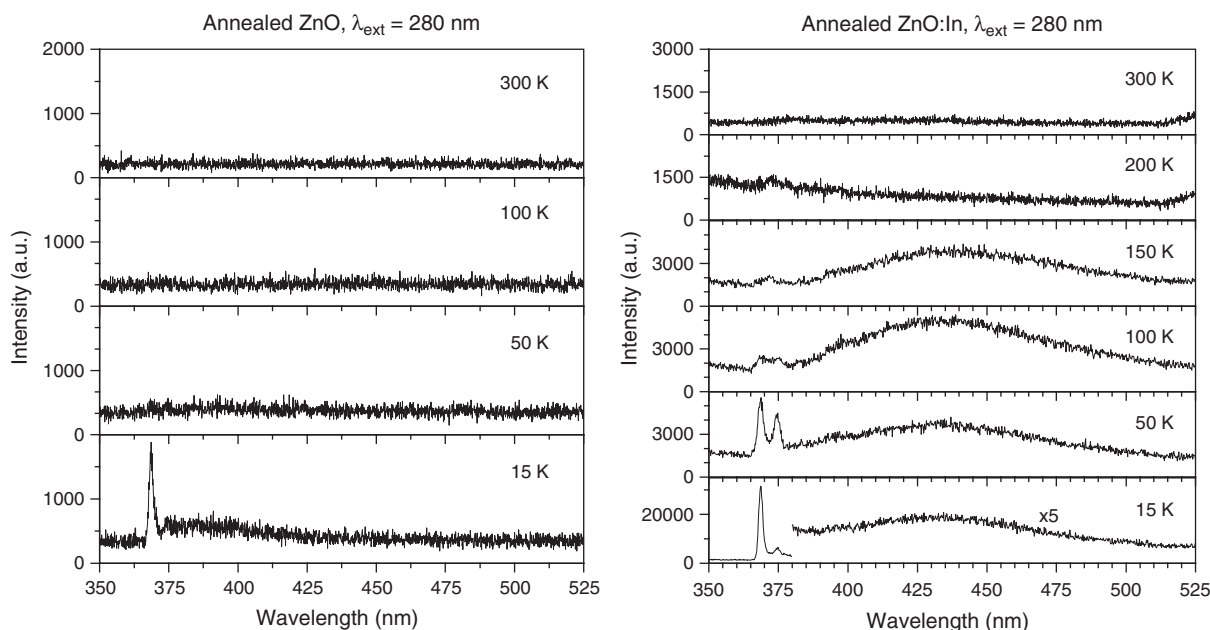


Fig. 3. Temperature dependence of (D^0,X) emission and blue emission bands in annealed zinc oxide nanostructures (excitation wavelength 280 nm).

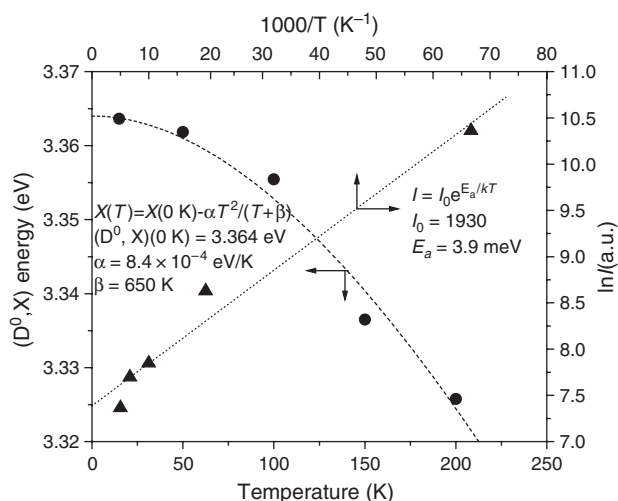


Fig. 4. Temperature dependence of (D⁰,X) emission intensity and its position for the annealed indium doped zinc oxide sample. Parameters used to generate the fittings are indicated.

the temperature range under study,²³ the bandgap energy E_g values of the Varshni's formula were substituted by the corresponding (D⁰,X) values. The Varshni's formula is expressed by the equation:

$$E_g(T) = E_g(0) - \alpha T^2 / (T + \beta) \quad (2)$$

where E_g is the bandgap energy, α and β are constants. The values employed in the curve-fitting were $\alpha = 8.4 \pm 0.3 \times 10^{-4}$ eV/K and $\beta = 650 \pm 40$ K (Fig. 4). The Varshni's expression gives an adequate prediction of the temperature dependence of the donor bound excitons and thus also the bandgap energy of ZnO. Wang and Giles²³ have measured the temperature dependence of free exciton (E_{XA}) energy, which also followed the Varshni's formula. The close similarity between our α and β values to the corresponding values for (E_{XA}) reported by Wang and Giles²³ ($\alpha = 8.2 \pm 0.3 \times 10^{-4}$ eV/K; $b = 700 \pm 30$ K) indicates that both bound and free excitons in ZnO have a similar temperature dependence.

Beside the characteristic UV emission of ZnO, a blue band is observed in Figure 3 with maximum at around 436 nm, which revealed an opposite temperature dependence behavior to the excitonic bands. Its intensity increases up to 100 K, showing even higher emission than the (D⁰,X) emissions; there after decreases and disappears completely beyond 150 K. This blue emission in ZnO has also been detected by several other researchers³²⁻³⁴ for ZnO thin films and assigned to the oxygen vacancy (V_o) and zinc interstitials (Zn_i). It must be noted that this blue emission is not very common in ZnO, and only observed when the samples are excited with short wavelengths. In our study we could observe this emission in the ZnO nanostructures only at low temperatures and with short excitation wavelengths like 280 nm. Zhang et al. could observe this emission in their ZnO

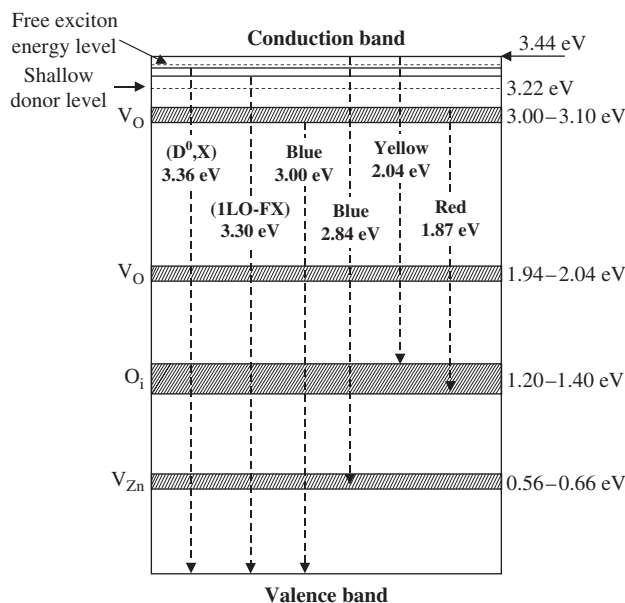


Fig. 5. Proposed energy band diagram for ZnO nanostructures at 15 K. The positions of the energy levels are given with respect to the position of the valence band.

thin films while exciting at 2701 nm.³² Oxygen vacancies in ZnO can produce two defect donor levels; the deep donor level located at 1.3–1.6 eV below the conduction band,^{35,36} and the shallow donor level about 0.3–0.5 eV below the conduction band.³⁴ The transition from the shallow donor level to the valence band is approximately at 2.8 eV, which corresponds to the position of the blue emission we observed. A proposed band diagram depicting the defect states in ZnO nanostructures at 15 K is illustrated in Figure 5. In fact from our EDS studies we observed that the incorporation of In in ZnO substitutes Zn atoms from their lattice sites.¹⁶ Thus, there might have some interstitial Zn atoms in the In doped sample, in

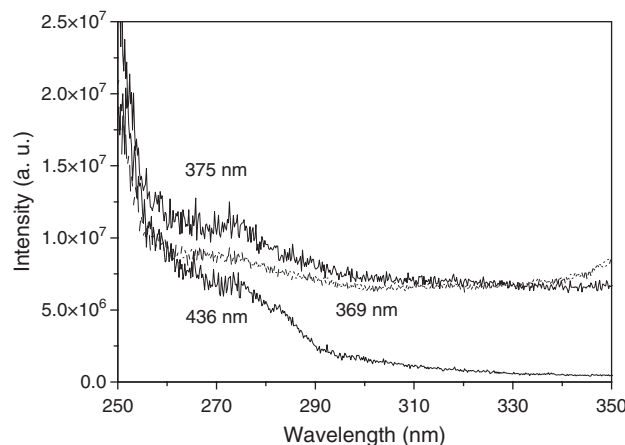


Fig. 6. Excitation photoluminescence (EPL) spectra from annealed indium doped ZnO at 15 K. The spectra correspond to (D⁰,X), ILO-FX and blue emission at 436 nm.

addition to some oxygen vacancies. Higher intensity of the blue emission in indium doped ZnO sample in comparison with the undoped one might be due to higher carrier population in V_o level due to the presence of shallow donor levels created by indium doping. Presence of shallow donor levels very close to the conduction band in indium doped ZnO nanostructures has been observed from our cathodoluminescence spectroscopic studies.²⁷

Figure 6 shows the EPL spectra of (D^0, X) (369 nm), 1LO-FX (375 nm) and the blue band (436 nm). In these spectra the baseline for the (D^0, X) and 1LO-FX emissions are not zero because of very close emission and excitation positions (Rayleigh scattering). From these spectra it can be noticed that the emissions located at 369 nm and 375 nm have similar features, with two very weak bands in the 260–290 and 300–330 nm regions. It is worth noting that the EPL spectrum of the blue emission differs from those of excitonic origin, mainly in the 275–290 nm region. The excitation band located around 283 nm indicates that the blue emission band indeed is related to localized electronic states induced by indium doping.

4. CONCLUSIONS

Low temperature photoluminescence measurements in undoped and indium-doped ZnO nanostructures revealed emission bands related to excitons bound to neutral donor (D^0, X), blue emissions related to shallow oxygen vacancy levels, yellow emission related to shallow and deep defect levels, and a red emission of DAP transition natures. On indium-doping, the intensity of both blue and yellow emissions increases in as-grown samples. While an increase of shallow donor levels below the conduction band due to indium doping is responsible for the increase of yellow emission intensity in indium doped sample (as-grown), an increase of carrier population in (V_o) levels from those shallow donor levels is possibly responsible for the enhancement of blue emission intensity in indium doped nanostructures. On thermal annealing, intensity of both blue and yellow emissions decreases for the doped and undoped samples.

Temperature dependence of (D^0, X) emission energy in ZnO nanostructures follows the Varshni's formula similar to the band gap energy. Close resemblance of the α and β values we calculated for the (D^0, X) emission and that of (E_{XA}) reported by Wang and Giles²² suggests that both bound and free excitons in ZnO have a similar temperature dependence. Rapid quenching of (D^0, X) intensity on increasing the temperature is due to weak binding between the excitons and donor defects at high temperatures.

Acknowledgments: We are thankful to E. Aparicio Ceja and I. Gradilla Martinez, CCMC-UNAM for their helps in XRD and SEM measurements of the nanostructures. The work is partially supported by CONACyT,

Mexico (grant No. 4626) and UC-MEXUS-CONACyT (grant No. CN-05-215). JZZ acknowledges the US Department of Energy for support.

References and Notes

1. K. Wang, R. W. Martin, K. P. O'Donnell, V. Katchkanov, E. Nogales, K. Lorenz, E. Alves, S. Ruffenach, and O. Briot, *Appl. Phys. Lett.* 87, 112107 (2005).
2. Y. F. Chen, D. M. Bagnall, V. Koh, K. Park, K. Hiraga, Z. Zhu, and T. Yao, *J. Appl. Phys.* 84, 3912 (1998).
3. W. Y. Liang and A. D. Yoffe, *Phys. Rev. Lett.* 20, 59 (1968).
4. A. E. Oberhofer, J. F. Muth, M. A. L. Johnson, Z. Y. Chen, E. F. Fleet, and G. D. Cooper, *Appl. Phys. Lett.* 83, 2748 (2003).
5. Ü. Özgür, Ya. I. Alivov, C. Liu, A. Teke, M. A. Reshchikov, S. Doğan, V. Avrutin, S.-J. Cho, and H. Morkoç, *J. Appl. Phys.* 98, 041301 (2005).
6. M. H. Huang, S. Mao, H. Feick, H. Yan, Y. Wu, H. Kind, E. Weber, R. Russo, and P. Yang, *Science* 292, 1897 (2001).
7. J. C. Johnson, H. Yan, R. D. Schaller, L. H. Haber, R. J. Saykally, and P. Yang, *J. Phys. Chem. B* 105, 11388 (2001).
8. D. C. Look, D. C. Reynolds, C. W. Litton, R. L. Jones, D. B. Eason, and G. Cantwell, *Appl. Phys. Lett.* 81, 1830 (2002).
9. P. Wang, N. Chena, Z. Yin, F. Yang, and C. Peng, *J. Cryst. Growth* 290, 56 (2006).
10. S. Y. Bae, C. W. Na, J. H. Kang, and J. Park, *J. Phys. Chem. B* 109, 2526 (2005).
11. Y. Yang, H. Yan, Z. Fu, B. Yang, and J. Zuo, *Appl. Phys. Lett.* 88, 191909 (2006).
12. S. A. Studenikin, N. Golego, and M. Cocivera, *J. Appl. Phys.* 84, 2287 (1998).
13. Z. K. Tang, G. K. L. Wong, P. Yu, M. Kawasaki, A. Ohtomo, H. Koinuma, and Y. Segawa, *Appl. Phys. Lett.* 72, 3270 (1998).
14. K. Vanheusden, W. L. Warren, C. H. Seager, D. R. Tallant, J. A. Voigt, and B. E. Gnade, *J. Appl. Phys.* 79, 7983 (1996).
15. A. B. Djurišić, Y. H. Leung, K. H. Tam, L. Ding, W. K. Ge, H. Y. Chen, and S. Gwo, *Appl. Phys. Lett.* 88, 103107 (2006).
16. A. Escobedo, M. Herrera, and U. Pal, *Opt. Mater.* 29, 100 (2006).
17. A. Teke, Ü. Özgür, S. Dogan, X. Gu, H. Morkoç, B. Nemeth, J. Nause, and H. O. Everitt, *Phys. Rev. B* 70, 195207 (2004).
18. K. Thonke, T. Gruber, N. Teofilov, R. Schönfelder, A. Waag, and R. Sauer, *Physica B* 308–310, 945 (2001).
19. C. Boemare, T. Monteiro, M. J. Soares, J. G. Guilherme, and E. Alves, *Physica B* 308–310, 985 (2001).
20. Y. S. Park, C. W. Litton, T. C. Collins, and D. C. Reynolds, *Phys. Rev.* 143, 512 (1966).
21. S. B. Zhang, S.-H. Wei, and A. Zunger, *Phys. Rev. B* 63, 075205 (2001).
22. Y. W. Chen, Y. C. Liu, S. X. Lu, C. S. Xu, C. L. Shao, C. Wang, J. Y. Zhang, Y. M. Lu, D. Z. Shen, and X. W. Fan, *J. Chem. Phys.* 123, 134701 (2005).
23. L. Wang and N. C. Giles, *J. Appl. Phys.* 94, 973 (2003).
24. E. de la Rosa, S. Sepúlveda-Guzman, B. Reesja-Jayam, A. Torres, P. Salas, N. Elizondo, and M. J. Yacamán, *J. Phys. Chem. C* 111, 8489 (2007).
25. X. L. Wu, G. G. Siu, C. L. Fu, and H. C. Ong, *Appl. Phys. Lett.* 78, 2285 (2001).
26. M. Liu, A. H. Kitai, and P. Mascher, *J. Lumin.* 54, 35 (1992).
27. M. Herrera, J. Valenzuela, U. Pal, and A. Escobedo, unpublished.
28. M. Gomi, N. Oorika, K. Ozaki, and M. Koyano, *Jpn. J. Appl. Phys.* 42, 481 (2003).
29. D. C. Look, J. W. Hemsky, and J. R. Sizelove, *Phys. Rev. Lett.* 82, 2552 (1999).
30. S. A. Studenikin, N. Golego, and M. Cocivera, *J. Appl. Phys.* 84, 2287 (1998).

31. Y. P. Varshni, *Physica (Amsterdam)* 34, 149 (1967).
32. D. H. Zhang, Z. Y. Xue, and Q. P. Wang, *J. Phys D: Appl. Phys.* 35, 2837 (2002).
33. L. Dong-Fang, T. Dong-Sheng, C. Li-Jie, Y. Xiao-Qin, L. Ying-Xin, Z. Zhen-Ping, Y. Hua-Jun, Z. Wei-Ya, and W. Gang, *Chin. Phys. Lett.* 20, 928 (2003).
34. Z. X. Fu, C. X. Guo, B. X. Lin, and G. H. Liao, *Chin. Phys. Lett.* 15, 457 (1998).
35. B. X. Lin, Z. X. Fu, and Y. B. Jia, *Appl. Phys. Lett.* 79, 943 (2001).
36. P. S. Xu, Y. M. Sun, C. S. Shi, F. Q. Xu, and H. B. Pan, *Chin. Phys. Lett.* 18, 1252 (2001).

Received: 18 November 2006. Accepted: 26 March 2007.